Temporally shaped femtosecond laser pulses as direct patterning method for dielectric materials in nanophotonic applications

Tamara Meinl[1], Nadine Götte[2], Yousuf Khan[1], Thomas Kusserow[1], Cristian Sarpe[2], Jens Köhler[2], Matthias Wollenhaupt[2,3], Arne Senftleben[2], Thomas Baumert[2] , Hartmut Hillmer[1]

[1]Institute of Nanostructure Technologies and Analytics, Technological Electronics and CINSaT, University of Kassel, Heinrich-Plett-Str. 40, 34132 Kassel, Germany
[2]University of Kassel, Institute of Physics and CINSaT, University of Kassel, Heinrich-Plett-Str. 40, 34132 Kassel, Germany
[3]Carl von Ossietzky University of Oldenburg, Institute of Physics, Carl-von-Ossietzky-Straße 11, 26111 Oldenburg, Germany

ABSTRACT

We present a direct patterning method of dielectric materials via temporally shaped femtosecond laser pulses. A thin-film waveguide with a 2D periodic pattern of photonic crystals with circular base elements is investigated. We use dielectrics since they are transparent especially in the visible spectral range, but also in UV and near infrared range. Thus, they are very suitable as optical filters in the very same spectral region. Since structuring of non-conductive dielectric materials suffers from charging, the implementation of laser processing as patterning method instead of conventional processing techniques like electron beam lithography or focused ion beams is a very attractive alternative. Despite a low refractive index contrast, we show by numerical results that normal incident of light to the plane of periodicity couples to a waveguide mode and can excite Fano resonances. That makes the device extremely interesting as narrow-band optical filter. Applications of optical filters in the visible and UV range require fabrication of photonic crystal structures in the sub-100 nm range.
Temporally shaped femtosecond laser pulses are applied as a novel method for very high precision laser processing of wide band gap materials to create photonic crystal structures in dielectrics. Shaping temporally asymmetric pulse trains enable the production of structures well below the diffraction limit.[1] We combine this process with deposition of a high refractive index layer to achieve the targeted resonant waveguide structure. Additionally, we focus on the rim formation arising by laser processing since this is an important issue for fabrication of photonic crystal arrays with small lattice constants.

KEYWORDS: Photonic crystal, guided-mode resonance, Fano filter, low refractive index contrast, dielectrics, fused silica, shaped femtosecond laser pulses, TOD, 3D FDTD, FIB

1. INTRODUCTION

Dielectric materials are transparent for UV, visible and near infrared light. Thus, they have great potential for usage in photonic devices. There is a big variety of dielectric materials available, e. g. oxides and nitrides, which offer good chemical and mechanical stability as well as good processing properties. Dielectrics offer a low-cost fabrication when compared to semiconductors but they underlie charging effects by conventional processing techniques based on electron beam lithography or focused ion beams like already presented in previous work.[2]
Temporally shaped femtosecond laser pulses as direct patterning method overcome those charging effects and additionally provide very fast processing time. Transparent dielectric materials become highly absorbing by applying ultrashort laser pulses with sufficient intensities, which enables material processing. Interaction between laser irradiation

Nanophotonics V, edited by David L. Andrews, Jean-Michel Nunzi, Andreas Ostendorf, Proc. of SPIE
Vol. 9126, 91262B · © 2014 SPIE · CCC code: 0277-786X/14/$18 · doi: 10.1117/12.2051749

and transparent materials is mainly based on deposition of energy into the medium to enable ablation of the material by plasma formation and the expansion of plasma into the material.[3,4,5] Generation of high free electron density is the key parameter to initiate this ablation process. The free electron density can be controlled by mainly two ionization processes, multiphoton and avalanche ionization.[6,7] Timescale and intensity of laser irradiation is decisive for the ionization processes and temporal evolution of free electron density.[8,9] Different experiments have shown that laser-induced damage threshold is strongly dependent on the laser pulse duration [10,11,12] and its temporal shape[6], respectively.
Furthermore, it has been demonstrated that direct structuring of dielectric materials with temporally asymmetric shaped femtosecond laser pulses generates reproducible structures being an order of magnitude below the diffraction limit (sub-100 nm structures).[1,6,13] In comparison to electron beam and focused ion beam techniques the laser structuring process has further advantages like abandonment of additional sample treatment and no vacuum conditions are required. Thus, laser-structured dielectric materials could become a remarkable tool for photonic applications.
We implement photonic crystal (PhC) structures and a waveguide layer with dimensions smaller than the targeted wavelength to enable the utilization of specific effects like guided-mode resonance effect. This effect is based on the interference of coupled leaky resonant waveguide modes and free space modes of direct reflection or transmission, respectively. So, externally propagating fields couple to modes of the waveguide.[14] The first model to describe these resonance types was designed by *Hessel and Oliner*[15] in 1965. Different approaches by using this effect as possible photonic applications have been reported. They vary from narrowband optical filters[14] over broadband reflectors[16] to polarizers[17]. Moreover, the utilization of the guided-mode resonance effect has also been demonstrated for asymmetric niobium pentoxide (Nb_2O_5) slabs[18], released silicon nitride membranes[19] and solid zirconium oxide (Zr_2O) wave guiding layers[2]. Consideration of fully solid slabs has not the potential of high refractive index contrast for good wave guiding than for example released membranes, but on the contrary they offer a stable composition, hence there is no residual stress.
We implement a periodic grating via shaped femtosecond laser pulses into a silicon oxide (SiO_2) substrate with refractive index (n_L) of around 1.5 and deposit a thin Nb_2O_5 layer with $n_H = 2.2$, acting as slab waveguide, to enable the coupling of incident light normal to the surface to discrete slab modes. Despite the low refractive index contrast we show that this device can be used as narrowband filters with asymmetric Fano resonances in the near infrared spectral region for structure sizes of typically a couple hundred nanometers. Those devices will be also applicable in the visible or UV spectral range simply by scaling down which results in structure sizes in the sub-100 nm-range.
In the following we give a brief overview about our numerical simulation method and the experimental setup. We introduce differently applied laser pulse shapes like bandwidth-limited, group delay dispersion (GDD) shaped and third order dispersion (TOD) shaped pulses to identify the best suitable pulse shape to produce our PhC structures. Structures generated with TOD shaped pulses are surveyed. The influence of the rim formation on the optical spectrum is simulated.

2. DESIGN & NUMERICAL SIMULATION METHOD

We are interested in dielectric device designs consisting of PhC structures which on the one hand are in general suitable to be used as optical filter designs and on the other hand possible in the technological fabrication process. We use finite difference time domain (FDTD) as modeling tool to characterize the interaction of light with our designed structures. The FDTD based open source software *meep*[20] is applied to model and simulate different designs of nanophotonic structures. *Meep* operates by solving Maxwell's equations calculating wave propagations as well as reflection and transmission spectra, respectively. The FDTD allows calculations in time domain using a broadband source with wide spectral range, such as a short Gaussian pulse.
The basic simulation principle is shown in Fig. 1. The simulation procedure of dielectric PhC waveguide uses periodic boundary conditions (PBC) in *x*- and *y*-direction where the PhC structure is repeated and perfectly matched layer (PML) boundaries are used in *z*-direction. We use a unit cell model for 3D-FDTD simulation of our dielectric PhC structures with a limited number of PhC holes in *x*- and *y*-direction. Instead of a full 3D model, the applied unit cell model is faster

due to its limited dimensions and consists of all the necessary information of the real device. An excitation source is placed normal to the plane of device and transmission and reflection flux monitor layers are placed below and above the waveguide layer, respectively. Full 3D simulations can additionally be performed to get more detailed information, but are not included in this work. The PhC structures with elliptical base elements of varying diameters d are arranged in a square lattice with lattice constant a. The influence of different waveguide layer thicknesses d_{wgl} was investigated. The discussed PhC devices in this publication have same waveguide layer thickness of $d_{wgl} = 330$ nm and same lattice constants $a = 1$ µm with elliptical holes in inner diameter $d = 500$ nm and $d = 660$ nm, respectively and depth $h = 900$ nm and $h = 1.66$ µm, respectively.

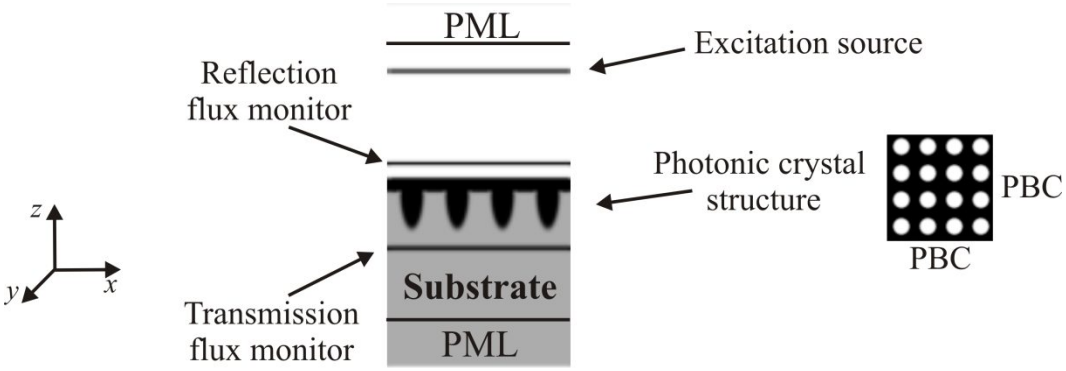

Figure 1: Basic composition of the simulation domain for the implemented PhC model. The domain is surrounded by PML boundaries in *z*-directions, while the model is repeated in *x*- and *y*-direction by applying periodic boundary conditions. A plane wave excitation source is placed normal to the surface. Reflection and transmission flux monitoring layers are placed above and below the PhC-layer, respectively.

The basic dielectric PhC structure composition is depicted in Fig. 2. The PhC material has a refractive index $n_H = 2.2$, which corresponds to the dielectric material Nb_2O_5 and the subjacent substrate (SiO_2) has the refractive index $n_L = 1.5$. Elliptical shaped base elements are traced back to the result of the fabrication process via focused ion beam lithography[1] as well as laser processing which will be shown later.

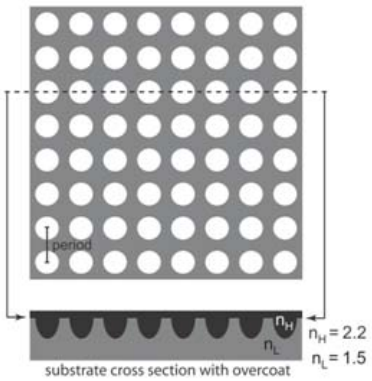

Figure 2: Composition of a dielectric PhC structure: Higher indexed waveguide layer (Nb_2O_5) with refractive index $n_H = 2.2$ and structured subjacent substrate (SiO_2) with $n_L = 1.5$.

3. EXPERIMENTAL SETUP & TECHNOLOGICAL FABRICATION

An amplified Ti:Sapphire laser system provides linearly polarized laser pulses with a full width at half maximum (FWHM) duration of 35 fs at a central wavelength of 800 nm. The laser setup for material processing is shown in Fig. 3 schematically. Laser pulses are temporally shaped with a home-built pulse shaper[21] and focused onto the substrate with microscope objective (OB) (*Zeiss LD Epiplan 50x/0.5*) of numerical aperture NA = 0.5 which corresponds to a lateral spot diameter of 1.4 µm ($1/e^2$ value of intensity profile[22]). The calculated spot diameter in axial direction of the $1/e^2$ intensity spread point function in air is 9.1 µm. A neutral density gradient filter (GF) is integrated to control the energy of the pulses which is monitored by a photodiode (PD) during the experiment. Confocal surface probing with a helium-neon laser is used for prepositioning of the substrate. The reflection from the surface is guided through a pinhole (PH) and focused by a lens (L) on a photomultiplier tube (PMT). The sample translation is motorized via a 3-axis piezo stage and provides an accuracy of 10 nm.

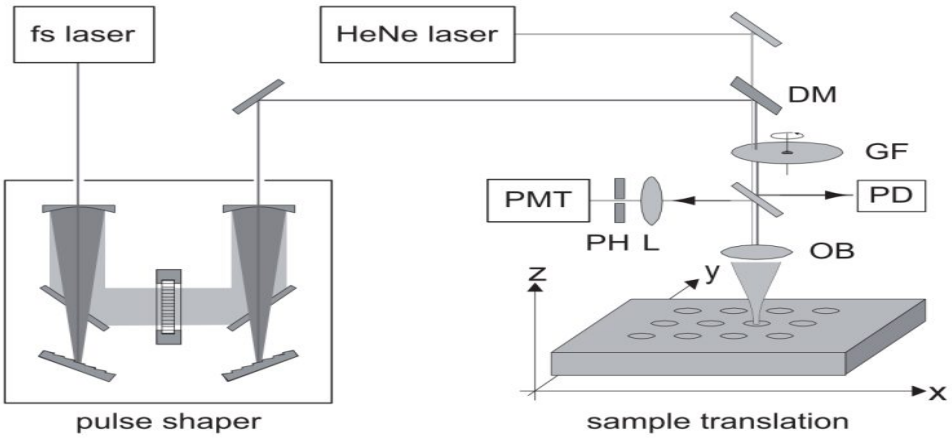

Figure 3: Experimental setup: Laser pulses are modulated via a home-built polarization pulse shaper and focused onto the substrate with a mircoscope objektiv of NA = 0.5 afterwards. A neutral density gradient filter (GF) is integrated o attenuate the energy of the laser pulses. The energy is monitored with a photodiode (PD) during experiment. A helium-neon laser which is coupled into the beam by a dielectric mirror (DM) is used for prepositioning. Sample translation is provided by 3-axis piezo stage.[1]

We investigate PhC hole profiles produced by bandwidth-limited and modulated femtosecond laser pulses. The latter are obtained by introducing group delay dispersion of $\varphi_2 = +1.5\times10^4$ fs^2 and third order dispersion of $\varphi_3 = +6\times10^5$ fs^3, respectively. TOD shaped pulse with positive φ_3 show a temporally asymmetric profile consisting of an intense sub-pulse followed by a long pulse train with a constant instantaneous frequency throughout the entire pulse. Whereas GDD shaped pulses with positive φ_2 show a temporally symmetric profile with a linearly increasing frequency (up-chirp).[1]
The focal position varies in vertical direction from a few micrometers below the substrate's surface to a few micrometers above in steps of $\Delta z = 1$ µm. The total energy of the pulses remains constant and structural changes can hence be investigated in relation to a varied focal position. Surface modifications resulting in rim formation are of particular interest in consideration of fabricating PhC array structures with decreasing lattice constants, where the melted zones would overlap.
Focused ion beam (FIB*) is used as analyzing method for characterization of the inner hole profiles. We perform cross-sectioning of the holes at their center to evaluate specifically the inner and outer hole diameter at the surface (d and D respectively) and inner diameter at a depth of 1 µm relative to surface (d_i) as well as width w_r and thickness d_r of the rim (refer Fig. 4). Since the dielectric material charges, we sputter a thin platinum layer as conductive layer to be able to

* *NVision40* from *Carl Zeiss*.

operate with FIB and SEM as this is the most versatile analyzing tool for the inner profile of our structures. An additional platinum layer is deposited locally on the hole structure to protect the structure from any damage while FIB milling process is running. After cross-sectioning, the hole profile parameters w_r, d_r, D, d and d_i shown in Fig. 4 are measured in SEM mode using the analyzing tool *SmartTiff* provided by *Zeiss*.

In future, the structured substrate will be coated with Nb_2O_5 waveguide layer using ion beam sputter deposition (IBSD) to realize the final filter device.

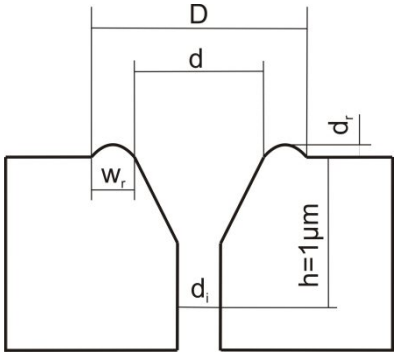

Figure 4: The hole profile parameters are: inner (d) and outer (D) hole diameter at the surface, inner diameter at a depth of 1 µm relative to surface (d_i), width (w_r) and thickness (d_r) of the rim.

4. RESULTS

As first result we present the hole profiles of differently shaped laser pulses to identify the best suitable pulse shape for structuring PhC's for nanophotonic applications. GDD and TOD shaped pulses show a similar hole profile, whereas the bandwidth-limited pulse is restricted in depth h by focusing directly onto the substrate surface. The hole profiles of the bandwidth-limited and modulated pulses for pulse energies 2.5 times above damage threshold are shown in Fig. 5 and the corresponding parameters are listed in Table 1. Structures generated with bandwidth-limited pulses exhibit an elliptical depth profile of around 340 nm. This results in an aspect ratio which is not sufficient to achieve strong guided-mode resonances.

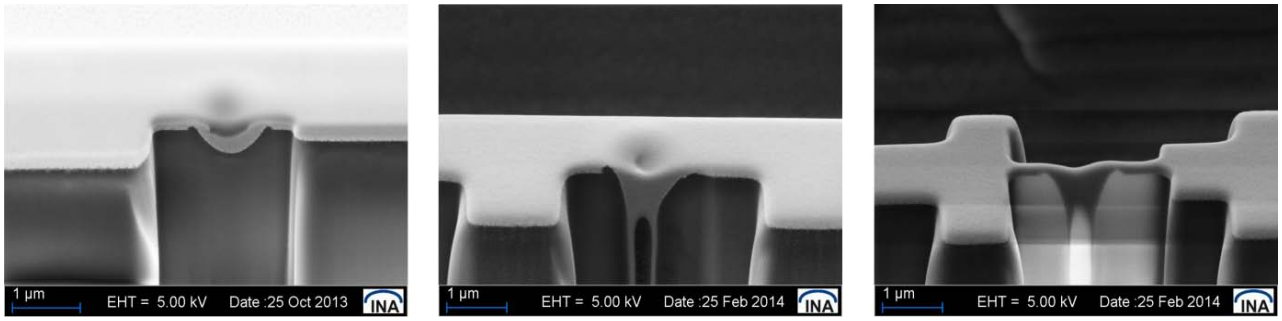

Figure 5: Resulting hole profiles from differently shaped laser pulses at the same focal position z = 0 µm at 2.5 times above damage threshold: bandwidth-limited pulse (left), GDD shaped pulse with $\varphi_2 = +1.5\times10^4$ fs^2 (center) and TOD shaped pulse with $\varphi_3 = +6\times10^5$ fs^3 (right).

Table 1: Hole profile parameters of the shaped pulses shown in Fig. 5. All values underlie an error of ±20 nm due to the analyzing software.

Pulse shape	Width of rim w_r [nm]	Thickness of rim d_r [nm]	Outer hole diameter D [µm]	Inner hole diameter d [nm]	Inner diameter (at h = 1 µm) d_i [nm]
Bandwidth-limited	140	64	1.253	956	-
GDD $\varphi_2 = +1.5\times10^4$ fs^2	223	138	1.668	1195	512
TOD $\varphi_3 = +6\times10^5$ fs^3	204	85	1.412	985	414

As demonstrated in Fig. 6 (left), the conical shape proves suitable for PhC structures for a narrowband filter. The numerical simulation Fig. 6 (right) is calculated with the parameters inner diameter d = 500 nm, depth h = 900 nm, lattice constant a = 1 µm and waveguide layer thickness d_{wgl} = 330 nm. Indeed, the simulated inner diameters are smaller than depicted in Fig. 5 but due to the funnel-formed upper structure, where the hole diameter decreases with increasing depth, it is a well compromise to get a first insight. Two sharp narrowband resonances can be observed at wavelengths around λ = 1.52 µm and λ = 1.82 µm. Moreover, an increase in diameter would consequently shift the resonance peaks to higher wavelength, but not inhibit the resonance itself. Furthermore, for application as guided-mode resonance filters in the visible spectral range structure sizes have to be scaled down.

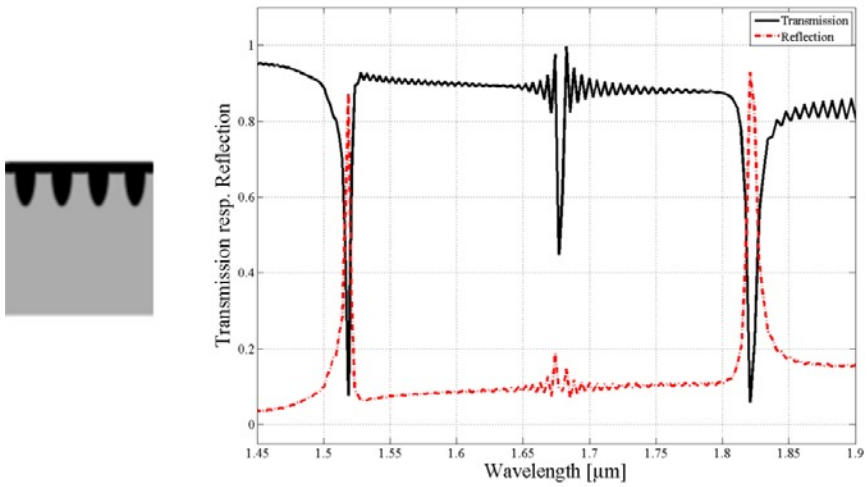

Figure 6: Numerical simulation parameters are: inner diameter d = 500 nm, depth h = 900 nm, lattice constant a = 1 µm and waveguide layer thickness d_{wgl} = 330 nm. Two sharp narrowband resonances appear at wavelength around λ = 1.52 µm and λ = 1.82 µm.

In the following we will discuss two more device designs produced by TOD shaped femtosecond laser pulses since the TOD shaped pulse shows a symmetric hole profile (Fig. 5 right) whereas the GDD pulse tends towards asymmetric funnel-formed profiles (Fig. 5 center). This is why we concentrate subsequently on structures generated with TOD shaped pulses. Figure 7 illustrates hole profiles fabricated with TOD shaped pulses with varying focal positions whose corresponding hole parameters are listed in Table 2. An enhanced rim formation is observable by focusing deeper into the substrate. Hole profiles whose focal position is above the surface show a decrease in the rim formation but the aspect ratio is not sufficient to provide strong guided-mode resonances (not shown).

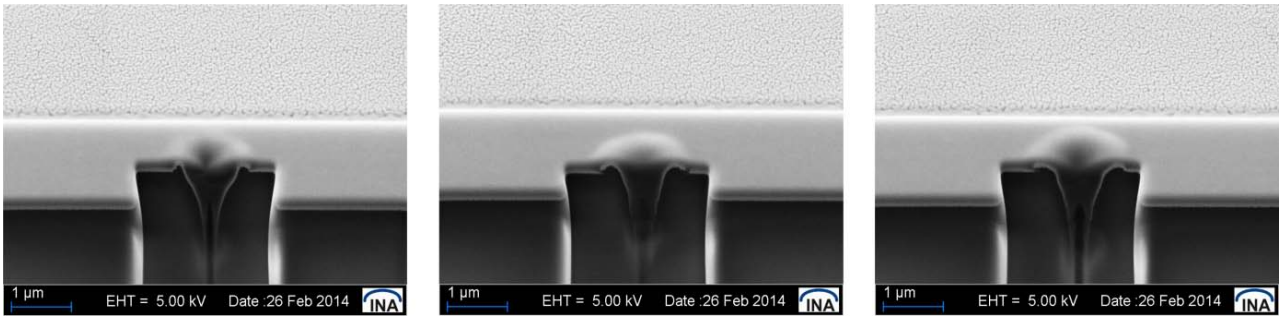

Figure 7: Resulting hole profiles from TOD ($\varphi_3 = +6\times10^5$ fs^3) shaped laser pulses with pulse energies 2.5 times above damage threshold. The focal position varies from 2 µm (left) and 1 µm (center) below surface and at surface (right), respectively.

Table 2: Hole profile parameters of the shaped pulses shown in Fig. 7. All values underlie an error of ±20 nm due to the analyzing software.

Focal position relative to the surface [µm]	**Width of rim w_r [nm]**	**Thickness of rim d_r [nm]**	**Outer hole diameter D [µm]**	**Inner hole diameter d [nm]**	**Inner diameter (at h = 1 µm) d_i [nm]**
-2	315	138	1.425	775	348
-1	315	85	1.517	860	328
0	191	99	1.287	887	243

The rim formation does not influence the optical spectrum very strongly which is observable in the numerical simulations (Compare Fig. 8 and Fig. 9). The resonance peak is slightly shifted, but has negligible influence as well on intensity as on FWHM of the spectral peaks.

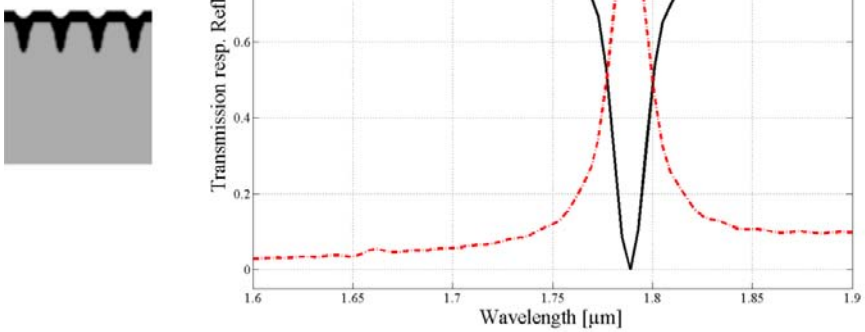

Figure 8: Numerical simulation parameters: inner diameter d = 660 nm, depth h = 1.16 µm, lattice constant a = 1µm and waveguide layer thickness d_{wgl} = 330 nm.

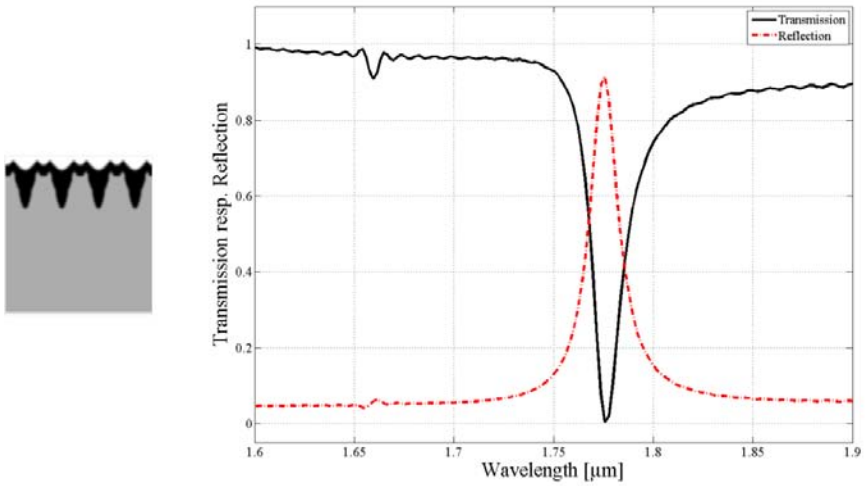

Figure 9: Numerical simulation parameters: inner diameter d = 660 nm, depth h = 1.26 µm, lattice constant a = 1 µm and waveguide layer thickness d_{wgl} = 330 nm. The rim formation is included and its influence on the optical spectrum is negligible; only a small blue-shift of the resonance peak is observable.

However, in consideration of processing a PhC array with decreasing lattice constants, rim formation can complicate positioning of the structures since the rims would overlap and influence each other in an unpredictable and uncontrollable way. Hence, we are currently working on technological possibilities to avoid or significantly reduce the rim formation by adding a very thin additional dielectric layer before the laser structuring process, so that the rim generation only takes place within this sacrificial layer which can be removed afterwards.

5. CONCLUSIONS & OUTLOOK

We presented numerical design solutions adapted to fabricated dielectric PhC structures fabricated with temporally shaped femtosecond laser pulses. Despite a low refractive index contrast of the dielectric materials we demonstrated numerically that those devices show great potential as narrowband optical filters due to guided-mode resonances. Furthermore, the analysis of the hole profiles confirms that material processing with temporally shaped femtosecond laser pulses as direct patterning method of dielectrics is a very promising tool for nanophotonic device fabrication. We presented the fabrication of hole profiles by three differently shaped laser pulses (bandwidth-limited, GDD and TOD). TOD shaped pulses are proved to be the best shaping technique for PhC structures required for guided-mode resonance filters, because they offer a good compromise concerning aspect ratio and rim formation. Regarding the rim formation, we are currently investigating possible solutions by adding a dielectric sacrificial layer to avoid or reduce this melting zone.

As following steps we will fabricate PhC array structures in the near infrared range with TOD shaped laser pulses and finalize it with the deposition of the waveguide layer to characterize the device optically regarding transmission and reflection spectrum, respectively. For the extension of the applicability to the visible and UV spectral range all parameters like hole diameter and lattice constant have to be downscaled.

ACKNOWLEDGEMENT

The research, performed at the Institute for Nanostructure Technologies and Analytics and the Institute of Physics, was funded by the *Deutsche Forschungsgemeinschaft* (DFG – German Research Foundation) in the priority program

"*SPP1327: Optisch erzeugte Sub-100-nm-Strukturen für biomedizinische und technische Applikationen*". Additionally, the authors thank Anita Dück for scientific and technical support.

REFERENCES

[1] Wollenhaupt, M.; Englert, L.; Horn, A. and Baumert, T. "Control of Ionization Processes in High Band Gap Materials," Journal of Laser Micro/Nanoengineering 4, 144-151 (2009)

[2] Kusserow, T.; Khan,Y.; Zamora, R.; Messow, F. and Hillmer, H., "Guided-mode resonances in dielectric photonic crystal slabs with low index contrast," Optical MEMS and Nanophotonics (OMN), 2012 International Conference, Technical digest, 170-171 (2012)

[3] Balling, P. and Schou, J. "Femtosecond-laser ablation dynamics of dielectrics: basics and applications for thin films" Rep. Prog. Phys. 76, 036502 (2013)

[4] Mao, S.S.; Quéré, F.; Guizard, S.; Mao, X.; Russo, R.E.; Petite, G. and Martin, P. "Dynamics of femtosecond laser interactions with dielectrics," Applied Physics A 79, 1695-1709 (2004)

[5] Vogel, A. and Venugopalan, V. "Mechanisms of Pulsed Laser Ablation of Biological Tissues," Chem. Rev. 103, 577-644 (2003)

[6] Englert, L, Rethfeld, B.; Haag, L.; Wollenhaupt, M.; Sarpe-Tudoran, C.; and Baumert, T. "Control of ionization processes in high band gap materials via tailored femtosecond pulses," Opt. Express 15, 17855-17862 (2007).

[7] Sarpe, C.; Köhler, J.; Winkler, T.; Wollenhaupt, M. and Baumert, T. "Real-time observation of transient electron density in water irradiated with tailored femtosecond laser pulses;" New Journal of Physics 14, 1367-2630 (2012)

[8] Rethfeld, B. "Unified model for the free-electron avalanche in laser-irradiated dielectrics," Phys. Rev. Lett. 92, 187401 (2004)

[9] Rethfeld, B. "Free-Electron Generation in Laser-Irradiated Dielectrics," Phys. Rev. Lett. 73, 035101 (2006)

[10] Stuart, B. C.; Feit, M. D.; Rubenchik, A. M.; Shore, B. W.; Perry, M. D. "Laser-Induced Damage in Dielectrics with Nanosecond to Subpicosecond Pulses," Phys. Rev. Lett.74, 2248-2251 (1995)

[11] Tien, A.C.; Backus, S.; Kapteyn, H.; Murnane, M. and Mourou, G. "Short-Pulse Laser Damage in Transparent Materials as a Function of Pulse Duration," Phys. Rev. Lett. 82, 3883-3886 (1999)

[12] Lenzner, M.; Krüger, J.; Sartania, S.; Cheng, Z.; Spielmann, Ch.; Mourou, G.; Kautek, W. and Krausz, F. "Femtosecond Optical Breakdown in Dielectrics," Phys. Rev. Lett. 80, 4076-4079, (1998)

[13] Englert, L.; Wollenhaupt, M.; Sarpe, C.; Otto, D. and Baumert, T. "Morphology of nanoscale structures on fused silica surfaces from interaction with temporally tailored femtosecond pulses," Journal of Laser Applications, 24, 042002 (2012)

[14] Magnusson, R. and Wang, S. S. "New principle for optical filters," Applied Physics Letters 61, 1022-1024 (1992)

[15] Hessel, A. and Oliner, A. A. "A New Theory of Wood's Anomalies on Optical Gratings," Appl. Opt. 4, 1275-1297 (1965)

[16] Boutami, S; Bakir, B; Hattori, H; Letartre, X.; Leclercq, J.-L.; Rojo-Romeo, P.; Garrigues, M.; Seassal, C. and Viktorovitch, P. "Broadband and Compact 2-D Photonic Crystal Reflectors with Controllable Polarization Dependence," IEEE Photonics Technology Letters 18, 835-837 (2006)

[17] Zamora, R.; Benes, M.; Kusserow, T.; Hillmer, H.; Akcakoca, U. and Witzigmann, B. "Optical Characterization of Photonic Crystals as Polarizing Structures for Tunable Optical MEMS Devices," Proc. IEEE Conference on Optical MEMS und Nanophotonics, 83-84 (2011)

[18] Nazirizadeh, Y.; Lemmer, U.; Gerken, Martina, "Experimental quality factor determination of guided-mode resonances in photonic crystal slabs," Applied Physics Letters 93,261110 (2008)

[19] Crozier, K.; Lousse, V.; Kilic, O.; Kim, S.; Fan, S. and Solgaard, O. "Air-bridged photonic crystal slabs at visible and near-infrared wavelengths," Physical Review B 73 (2006)

[20] Oskooi, A. F., Roundy, D., Ibanescu, M., Bermel, P., Joannopoulos, J. and Johnson, S. G. "Meep: A flexible free-software package for electromagnetic simulations by the FDTD method," Computer Physics Communications 181, 687-702, (2010)
[21] Köhler, J.; Wollenhaupt, M.; Bayer, T.; Sarpe, C. and Baumert, T. "Zeptosecond precision pulse shaping," Optics Express 19, 11638-11653 (2011)
[22] Gu, M. [Advanced optical imaging theory], Springer-Verlag, Berlin, 2000